FINITE ELEMENT SIMULATIONS OF THE SWIFT EFFECT

L. Duchêne[1], F. El Houdaigui[2], A. M. Habraken[2]
[1]COBO Department, Royal Military Academy, Belgium;
[2]Department of Mechanics of Materials and Structures, University of Liège, Belgium

Summary

Numerical simulations of the experimental free-end torsion tests [1] of copper cylindrical bars were analysed in the present paper. The self-made Finite Element (FE) code Lagamine with polycrystal plasticity models computed numerical prediction of the Swift effect, i.e. the lengthening of the cylinder during the torsion. The used constitutive law was coupled with two plastic crystal models, taking or not into account strain rate effect. Results such as axial strain and predicted textures were analysed. The ones obtained for shear strains lower than 1.0 were in good agreement with experiments; while, for shear strains larger than 1.0, the FE results were currently unfair. A research about remeshing is in progress to improve the accuracy of the results for large shear strains.

Keywords: Swift effect, free-end torsion, Taylor's model, texture

1 Introduction

The Swift effect has first been observed in 1947 [2]. It refers to the lengthening or shortening of a cylinder submitted to torsion. In fact, the geometry of the sample can either be a cylinder or a tube. Under large plastic torsional strains, their length varies.
According to [2], the Swift effect has its origin in the interaction between crystals with different orientations. Slip system activity based plasticity and rotation of the crystal lattice are also crucial points.
The shear strain, which measures the torsion, can be defined by different ways according to literature. For instance, 4 definitions of shear strain are presented in [3]. The following one (proposed and recommended by [3]) is used in the present paper:

$$\gamma = \frac{r\Phi}{l_0} = r\Psi \qquad (1)$$

where r is the current radius, Φ is the twist angle, l_0 is the initial length and Ψ is the twist angle per unit initial length of the cylinder or the tube.
Several parameters influence material behaviour: lengthening or shortening of the bar during torsion. Toth's studies showed very large influence of initial texture of the material during torsion of thin-walled copper tubes and copper wires respectively in [4] and [5]. The effect of sample temperature during the torsion of copper bars was analysed in [1]. Lengthening was observed during the torsion at room temperature and

125°C. Lengthening followed by shortening appeared for higher temperatures (200°C and 300°C). By analysing the texture of the sample at different shear strains, it appeared that dynamic recrystallization occured for the higher temperatures. This dynamic recrystallization was at the origin of the shortening behaviour observed in [1].
On the numerical point of view, several models have been investigated for the Swift effect prediction (see **Table 1** for references). According to [3] and [4], the strain rate sensitivity has a very large influence on the Swift effect. [3] observed lengthening for low values of strain rate sensitivity ($m<0.13$), shortening for high values ($0.167<m<1$) and lengthening followed by shortening for intermediate values of m.

Table 1: *Elongation strains reported in the literature*

Shear strain (%)	Elongation strains (%)	Methods used	Materials investigated	Ref.
up to 500	from 1 to 11	experimental	70-30 brass, stainless steel, aluminium, cupro-nickel, copper, mild steel and 0.5% carbon steel.	[2]
260	7	experimental	304L stainless steel	[6], [7]
280	6.8 (experiment) 10 (numerical)	experimental and analytical* elastic-perfectly plastic and kinematic hardening plastic models	thin-walled metal tubes	[8]
40 to 60	0.4 to 0.8	experimental	iron and steel	[9]
50	1.5	analytical* model based on [10]	aluminium	[11]
150	≈10	torsion dedicated FE analysis with Taylor-type polycrystal plasticity and sophisticated hardening models	70-30 brass	[12]
15	from –1.5 to +1.5 depending on the texture	experiments from [13] and two analytical* models: rate sensitive and continuum mechanics of textured polycrystals	thin-walled copper tubes	[4]
up to 2000	from –35 to +50 depending on the strain rate sensitivity	analytical* rate sensitive crystal plasticity model of the Sachs type	initially isotropic material	[3]
up to 500	from –4 to 3 depending on the annealing temperature	experimental and analytical* rate sensitive polycrystal Sachs model	copper wires	[5]
up to 1200	up to 5.5	experimental	copper bars	[1]

*analytical model means that torsion is imposed analytically (without FE analysis).

Elongation strains have been measured experimentally and predicted numerically by several authors (Swift, Miller, Xiao, Toth, Jonas, Neale…) for different materials. **Table 1** summarizes the elongation strains and the corresponding shear strains found in literature.
The experimental Swift effect measurements presented in [1] are investigated in this paper. The FE code Lagamine (developed at the M&S department since 1984; see [14,15,16,17] for some applications of this code) coupled with a crystal plasticity model (described in section 2) was applied to provide numerical simulations of free-end torsion of copper bars.

2 Description of the finite element constitutive law

It is well-known that plastic deformation of polycrystalline material induces reorientation of individual grains into preferred orientations. This phenomenon, i.e. the texture evolution, is responsible for induced mechanical anisotropy of material, which plays an important role in forming processes. The implementation of texture evolution into FE codes is therefore of great importance. Unfortunately, micro-macro models generally require very long computation time and large memory storage.
These considerations led us to the development of a local yield locus approach able to predict texture evolution during FE modelling of industrial forming processes. With this model, only a small zone of the yield locus is computed. This zone is updated when its position is no longer located in the part of interest in the yield locus or when the yield locus changes due to texture evolution.
This local yield locus approach has already been validated and extensively used to model deep drawing processes (see [18] and [19] for details).
This model is specific in the sense that it does not use a yield locus formulation either for plastic criterion or in the stress integration scheme. A linear stress-strain interpolation in the five-dimensional (5D) stress space described by equation (2) is used at the macroscopic scale:

$$\underline{\sigma} = \tau \underline{\underline{C}} \bullet \underline{u} \qquad (2)$$

In this equation, $\underline{\sigma}$ is a 5D vector containing the deviatoric part of the stress; the hydrostatic part being elastically computed according to Hooke's law. The 5D vector $\underline{u}$ is the deviatoric plastic strain rate direction (it is a unit vector). τ is a scalar describing the work hardening according to the exponential relationship of equation (3) where the strength coefficient K, the offset Γ^0 and the hardening exponent n are material parameters fitted on experimental data and Γ is the polycrystal induced slip.

$$\tau = K \cdot \left(\Gamma^0 + \Gamma\right)^n \qquad (3)$$

The macroscopic anisotropic interpolation is included in matrix $\underline{\underline{C}}$ of equation (2). Its identification relies on 5 directions: $\underline{u}_i$ (i=1…5) advisedly chosen in the deviatoric strain rate space and their associated deviatoric stresses: $\underline{\sigma}_i$ (i=1…5) computed by the polycrystal plasticity model. This micro-macro model uses in fact Taylor's assumption of equal macroscopic strain and microscopic crystal strain. It computes the average of

the response of a set of representative crystals evaluated with a microscopic model taking into account the plasticity at the level of the slip systems. In this paper, two versions of this Full Constraints (FC) Taylor's model are investigated: one coupled with a rate insensitive crystal plastic model and one coupled with a visco-plastic crystal model. The stress vectors $\underline{\sigma_i}$ lie on the yield locus. They define the vertices of the interpolation domain and are called 'stress nodes'. The $\underline{\underline{C}}$ matrix is built on the basis of these 5 stress nodes.
With this method, only a small part of the yield locus is known. As long as the interpolation is achieved in the domain delimited by these 5 stress nodes, the interpolation matrix $\underline{\underline{C}}$ is valid. When the stress direction explored during FE computation falls out of this domain, updating of the stress nodes must take place; a new interpolation matrix is then computed.
Texture evolution is computed using Taylor's model on the basis of the strain history for each integration point every 10 FE time steps. $\underline{\underline{C}}$ matrix must be updated when texture evolution occurs.
The above considerations are sufficient to understand the basic concepts of the local yield locus implemented in Lagamine code. Further details and properties of such parameterisation of a N dimensional space have been investigated in [18] and [19].

3 Finite element simulation of free-end torsion

Experimental free-end torsion of copper cylinders have been investigated in [1]. The samples were 8 mm long and their radius was 3.2 mm. The torsion was achieved up to shear strains γ of 12 (at the surface of the cylinders) at different temperatures ranging from room temperature to 300°C.
The goal of this paper is to reproduce numerically the observations of [1] in terms of length changes and texture evolution. In order to avoid dynamic recrystallization observed at high temperature (and not modelled in our simulations), the experimental results at room temperature are focussed on.
The FE mesh consisted of 12 layers (along the axial direction) of 128 elements. This yielded to a total of 1536 BWD3D elements. These are new developed finite elements recently implemented in the FE code Lagamine. They are based on the non-linear three-field (stress, strain and displacement) HU-WASHIZU variational principle [20]. A first feature of the BWD3D element is a new shear locking treatment based on the recent Wang-Wagoner method (see [21]). This method identifies the hourglass modes responsible of the shear locking and removes them. The second feature of this new element is the use of a corotational reference system. This is made necessary for the identification of the hourglass modes. A grateful consequence of this corotational reference system is a simple and accurate treatment of the hourglass stress objectivity.
The comparison of the results obtained with the BWD3D element with the results of a former version of this element: the BLZ3D [22] (see **Figure 1**) proves the large importance of the accuracy of the element formulation and in particular the shear locking treatment.
The torsion was imposed in the FE code by fixing the lower node layer and by twisting progressively the upper node layer. In order to model the free-end torsion, the axial

degree of freedom of the twisted nodes remained free.
Material parameters used in the FE code corresponded to the material exploited in [1]: Young's modulus was 130 GPa, Poisson's ratio was 0.34. The hardening behaviour was described by equation (3) with the parameters: K=82.7, Γ^0=0.0049 and n=0.2208. The initial texture of the samples has been experimentally measured. It presented a cylindrical symmetry (due to the bar forming processes) and a weak anisotropy. The 12 slip systems {1 1 1}<1 1 0> typical for fcc materials were used in the crystal plasticity models.

4 Results

4.1 Length changes

Figure 1 presents the length change, i.e. the Swift effect, as a function of the shear strain linked to the torsion (and defined by equation (1)). FE results obtained with the BLZ3D and the BWD3D elements are compared with experimental results [1]. The effects of texture evolution and strain rate sensitivity are also presented. Finally, results obtained analytically (without FE method) by [23] using the Taylor visco-plastic polycrystal model are plotted. Equilibrium equation and zero axial force were imposed to model the free-end torsion.
As explained in section 3, the BLZ3D element did not yield to satisfactory results. For shear strains larger than 0.5, the lengthening diminished abnormally. The formulation of this element is not able to model accurately the free-end torsion for large shear strains because of inadequate solution for shear locking and inaccurate hourglass stress objectivity.

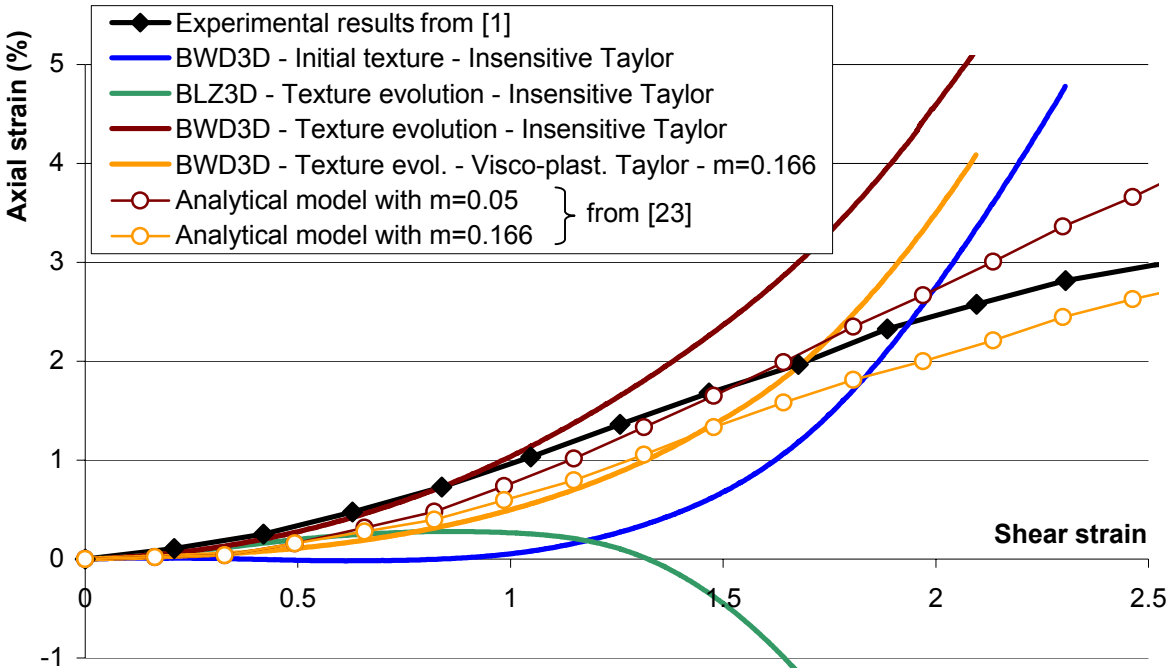

Figure 1: *Axial strain versus shear strain during free-end torsion.*

Using the BWD3D element, results obtained with the local yield locus constitutive law (see section 2) with computation of texture evolution were in very good accordance with experimental curve for shear strains up to 1.0. But, for larger shear strains, the lengthening was overestimated.
When the initial texture was used throughout the simulation, no lengthening was observed for shear strain up to 1.0. For larger shear strains, a rapid increase of the axial strain appeared. This unexpected behaviour is certainly due to an inaccuracy at large strains of our 3D FE mesh. Indeed, if the initial texture does not yield to a Swift effect at small strains, it should not yield to lengthening for larger shear strains.
The effect of polycrystal plasticity model can be visualized by comparing the strain rate insensitive Taylor's model with the visco-plastic Taylor's model. The viscous effect tended to reduce the amplitude of the Swift effect. Such an effect of strain rate sensitivity has already been analysed by several authors (see for instance [3,4,23]). Indeed, analytical results [23] are in agreement with FE method; especially in the case m=0.166. The analytical results with m=0.05 (very low value) can be compared with FE method using the insensitive Taylor's model, but the agreement is worse.

4.2 Texture evolution

As the texture and particularly the texture evolution are crucial points for the Swift effect, the predicted textures were analysed. **Figure 2** compares the predicted texture with the measured one on a deformed sample for a shear strain of 2.0. {1 1 1} pole figures were investigated as is usual for shear textures.
The texture obtained for a shear strain of 2.0 are quite different from the initial texture. Texture evolution was then very important to be taken into account. **Figure 2** shows that the agreement between the predicted and the measured textures is quite good (qualitatively as well as quantitatively). The shift observed between the horizontal axis and the maximum of the pole figures was also modelled by FE simulation.

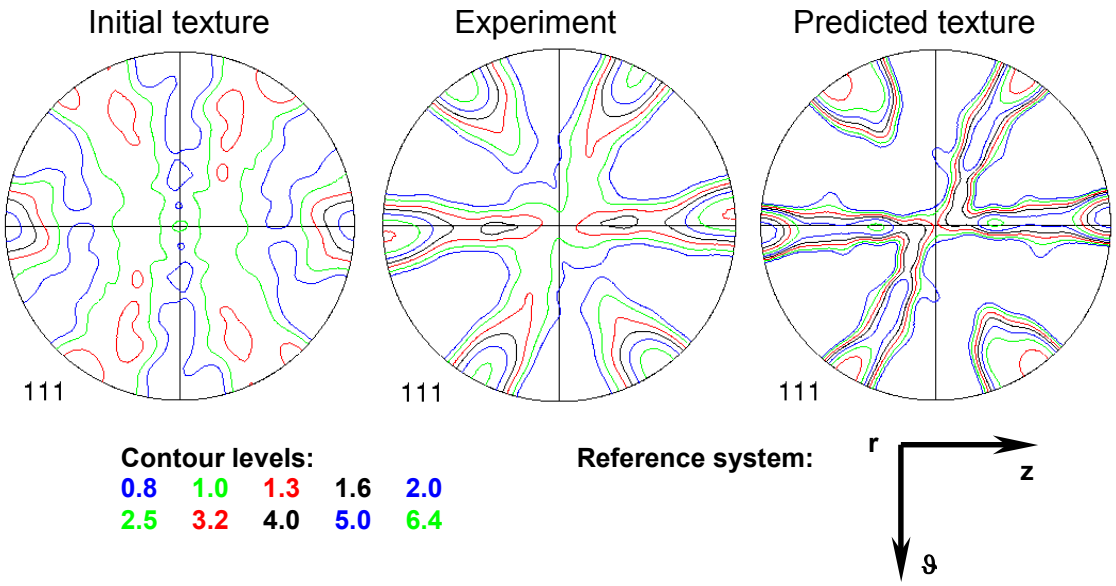

Figure 2: *Final textures for a shear strain of 2.0 in {1 1 1} pole figures.*

A shift of 4° in the sense opposite to the shear direction can be measured on the experimental pole figure while a value around 2.5° was predicted. As detailed in [1], this shift is very important and closely linked to the Swift effect.

5 Conclusions

In this paper, the experimental results of [1] for free-end torsion of copper bars were predicted with polycrystal plasticity models implemented in the FE code Lagamine. Predicted Swift effect (axial lengthening) as a function of shear strain (see **Figure 1**) was in very good agreement with experimental results for shear strains lower than 1.0: the case without texture evolution did not exhibit lengthening; the case with the strain rate insensitive Taylor's model and texture evolution was almost superimposed to experimental results (for $\gamma<1.0$); while the case with a strain rate sensitivity m=0.166 was lower (as has also been observed by [23]). This proves the ability of our model to predict the Swift effect.
Texture evolution must be taken into account for Swift effect prediction. The shift from the ideal orientation observed on the pole figures of **Figure 2** is identified to be related to the lengthening of the cylinder (see [1]). As this shift was reproduced correctly with the FE method, Swift effect should also be reproduced correctly. However, for shear strains larger than 1.0, accuracy of 3D FE results became very poor. Distortion of the finite elements is expected to be at the origin of the inaccuracy. Remeshing of the cylinder will therefore be investigated to improve results obtained with FE model up to large shear strains. Even if carrying out 3D FE computation seems complicated compared with analytical models, a great advantage of FE models is their large adaptability. Complex geometries, complex texture distributions can therefore be investigated.

Acknowledgements

A. M. Habraken is mandated by the National Fund for Scientific Research (Belgium). Professor Paul Van Houtte is acknowledged for providing us with texture treatment modules. The authors acknowledge Professor Laszlo Toth for the experimental data and the visco-plastic Taylor's model. The authors also thank the Belgian Federal Science Policy Office (Contract P5/08) for its financial support.

References

[1] Toth, L.S., Jonas, J.J., Daniel, D., Bailey, J.A.: Texture development and length changes in copper bars subjected to free end torsion, Textures and Microstructures 19 (1992), pp. 245-262.
[2] Swift, H.W.: Length changes in metals under torsional overstrain, Engineering 163 (1947) 253-257.
[3] Toth, L.S., Jonas, J.J., Gilormini, P., Bacroix, B.: Length changes during free-end torsion: a rate sensitive analysis, Int. J. of Plasticity 6 (1990), 83-108.

[4] Toth, L.S., Jonas, J.J.: Analytic prediction of texture and length changes during free-end torsion, Textures and Microstructures 10 (1989), pp. 195-209.
[5] Toth, L.S., Szaszvari, P., Kovacs, I., Jonas, J.J.: Shortening behaviour of twisted copper wires, Textures and Microstructures, Special issue ICOTOM 9, Guest Editors R. Penelle and C. Esling, 14-18 (1991), pp. 995-1000.
[6] Miller, M.P., McDowell, D.L.: Modeling large strain multiaxial effects in fcc polycrystals, Int. J. Plast., 12(7) (1996) 875-902.
[7] Miller, M.P., McDowell, D.L.: The effect of stress-state on the large strain inelastic deformation behavior of 304L stainless steel, ASME J. Engng. Mater. Technol. 118 (1996) 28-36.
[8] Xiao, H., Bruhns, O.T., Meyers, A.: Large strain responses of elastic-perfect plasticity and kinematic hardening plasticity with the logarithmic rate: Swift effect in torsion, Int. J. Plast. 17 (2001) 211-235.
[9] Rohatgi, A., Jonas, J.J., Shrivastava, S.: Effect of stress-relief annealing on the inverse Swift effect in steel and iron, Script. Metal. Mater. 32(5) (1995) 737-741.
[10] Hill, R.: A theory of the yielding and plastic flow of anisotropic metals, Proc. Roy. Soc., London A193 (1948) 281-297.
[11] Wu, H.C.: On finite plastic deformation of anisotropic metallic materials, Int. J. Plast. 19 (2003) 91-119.
[12] Wu, P.D., Neale, K.W., Van der Giessen, E.: Simulation of the behaviour of fcc polycrystals during reversed torsion, Int. J. Plast. 12(9) (1996) 1199-1219.
[13] Rose, W., Stüwe, H.P., Z. Metallkde 59 (1968), 396.
[14] Habraken, A.M., Charles, J.F., Wegria, J., Cescotto, S.: Dynamic recrystallization during zinc rolling, Int. J. of Forming Processes 1 (1998).
[15] Castagne, S., Pascon, F., Bles, G., Habraken, A.M.: Developments in finite element simulations of continuous casting, J. de Physique IV 120 (2004), pp. 447-455.
[16] Duchêne, L., Godinas, A., Cescotto, S., Habraken, A.M.: Texture evolution during deep-drawing processes, J. of Materials Processing Technology 125-126 (2002), pp. 110-118.
[17] Habraken, A.M., Cescotto, S.: An automatic remeshing technique for finite element simulation of forging processes, Int. J. Numerical Methods in Engineering 30 (1990), pp. 1503-1525.
[18] Duchêne, L.: FEM study of metal sheets with a texture based, local description of the yield locus, Ph. D. Thesis, Ulg, Liège, Belgium (2003).
[19] Habraken, A.M., Duchêne, L.: Anisotropic elasto-plastic finite element analysis using a stress-strain interpolation method based on a polycrystalline model, Int. J. of Plasticity 20, Issue 8-9 (2004) 1525-1560.
[20] Simo, J.C., Hughes, T.J.R.: On the variational foundations of assumed strain methods, J. Appl. Mech., ASME, 53 (1986) 51-54.
[21] Wang, J., Wagoner, R.H.: A New Hexahedral Solid Element for 3D FEM Simulation of Sheet Metal Forming, Proc. 8th int. conf. NUMIFORM 2004.
[22] Zhu, Y.Y., Cescotto, S.: Transient thermal and thermomechanical analysis by F.E.M., Comput. Struct. 53(2) (1994) 275-304.
[23] Qods, F., Toth, L.S., Van Houtte, P.: Modelling of length changes and textures during free end torsion of cylindrical bars, Proc. ICOTOM 14 (2005), to appear.